Planetary climate systems

Inner edge of habitable zone

- Runaway greenhouse limit
  Complete evaporation of ocean
- Water loss limit
  Escape of water/hydrogen to space

→ How/when did **Venus** lose water and get the thick CO_2 atmosphere ?

Outer edge of habitable zone

- Greenhouse effect by CO_2 and other gases
- Enhancement of cloud albedo in cold, massive atmospheres

→ How/when did **Mars** lose thick atmosphere and freeze ?

Runaway greenhouse effect

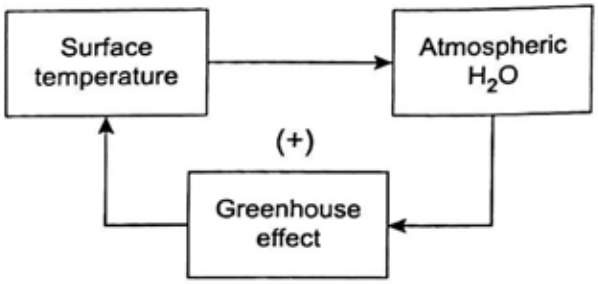

Figure 13.7 Diagram illustrating the positive feedback loop caused by water vapor.

Catling & Kasting (2017)

- An increase in surface temperature causes an increase in atmospheric water vapor, which then increases the greenhouse effect, causing a further increase in surface temperature. (Positive feedback)
- A wet atmosphere makes spectral atmospheric windows close up, and thermal infrared radiation cannot escape to cool the planet. If the absorbed solar flux exceeds the outgoing infrared limit, the surface water totally evaporates and the planet's surface heats up.

Runaway/moist greenhouse of early Venus

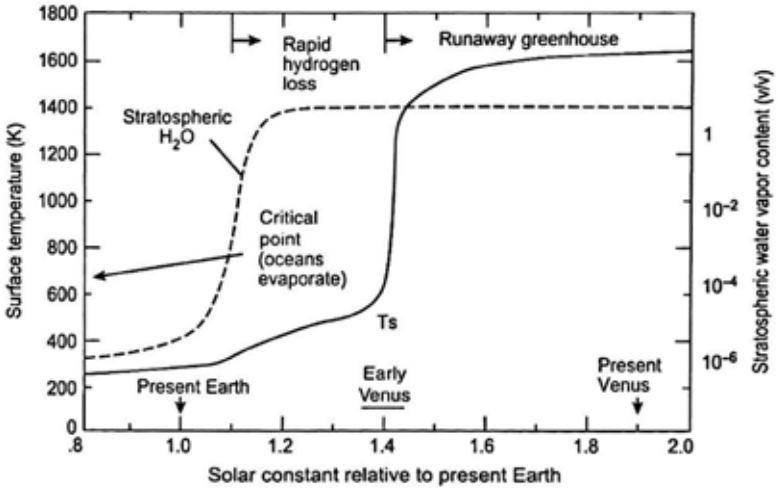

Albedo = 0.22 is assumed

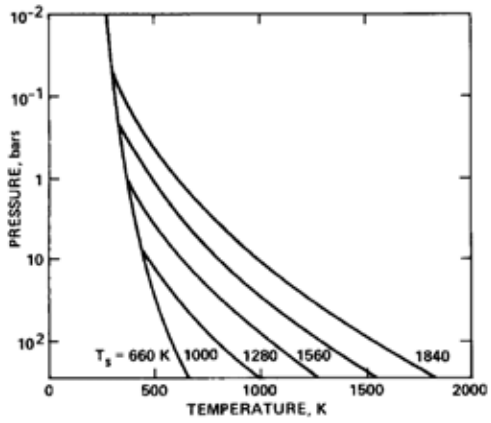

FIG. 6. Temperature versus pressure for selected runaway greenhouse atmospheres. The lower portions of the curves represent dry adiabats. The curve(s) to which they are all joined are moist pseudoadiabats, which are very nearly equivalent to the saturation vapor pressure curve for water.

Kasting 1988; Catling & Kasting 2017

Atmospheric structure in moist greenhouse
(Kasting 1988)

High H_2O mixing ratio in the upper atmosphere
→ Rapid hydrogen escape

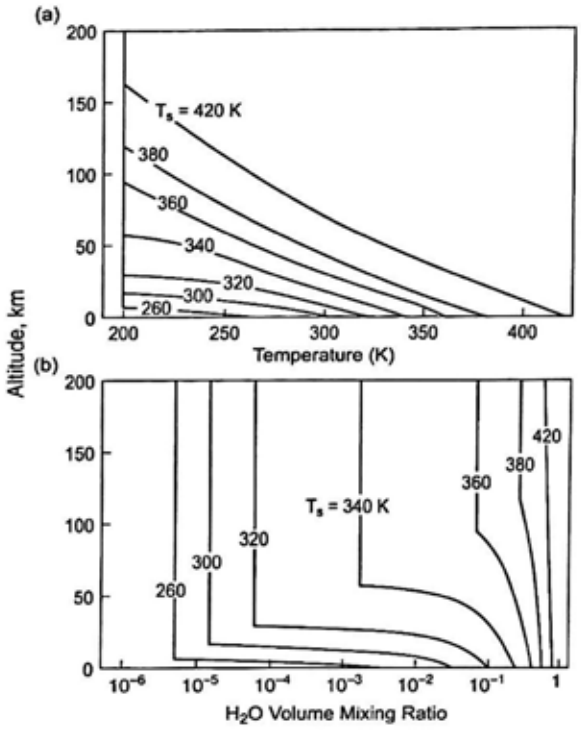

Figure 13.13 Vertical profiles of temperature (a) and water vapor mixing ratio (b) for atmospheres with different surface temperatures, T_s. A 1-bar N_2/O_2 background atmosphere is assumed. (From Kasting, (1988). Reproduced with permission from Elsevier. Copyright 1988.)

STRONG DEPENDENCE OF THE INNER EDGE OF THE HABITABLE ZONE ON PLANETARY ROTATION RATE (Yang et al. 2014, ApJ)

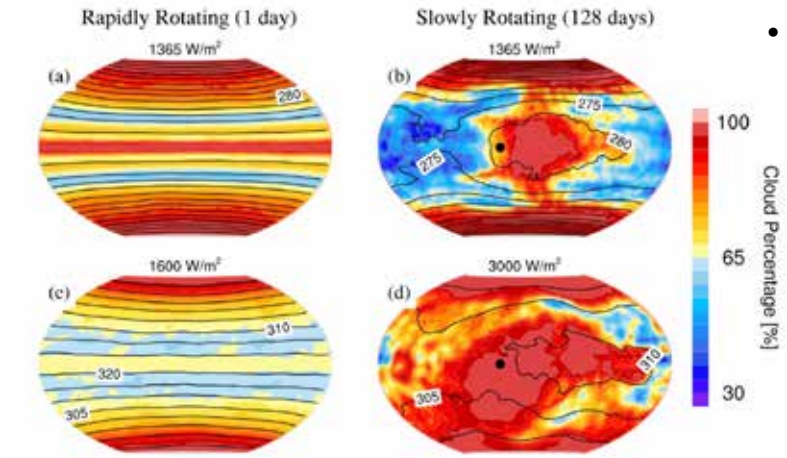

- Atmospheric circulation affects the albedo
- subsolar-to-antisolar circulation on slow rotators can generate thick clouds on the illuminated side

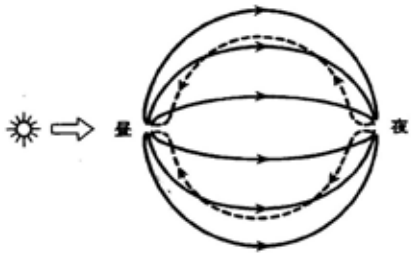

subsolar-to-antisolar circulation
(Y. Matsuda)

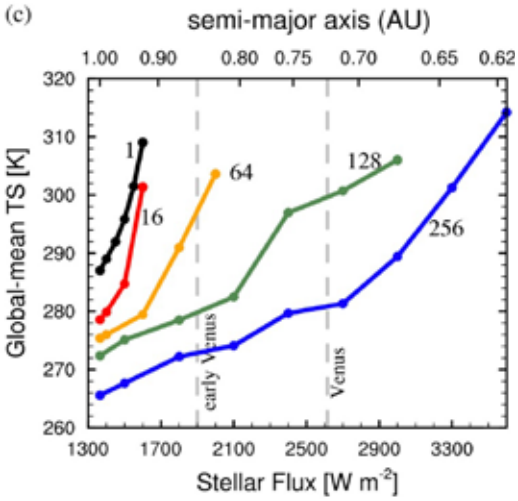

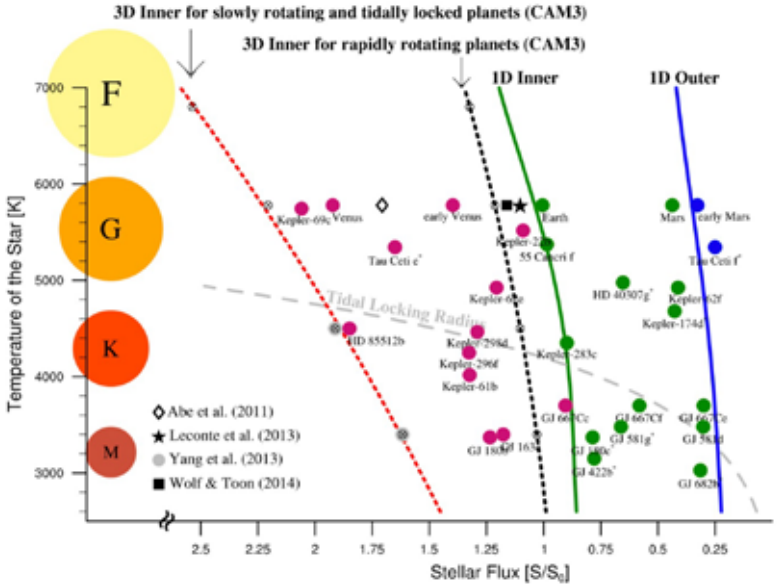

"Was Venus the first habitable world of our solar system?"

Way et al. (2016)

(Sim A) Solar flux: 1.46 x Earth, Rot. period: Modern Venus

Surface air temperature

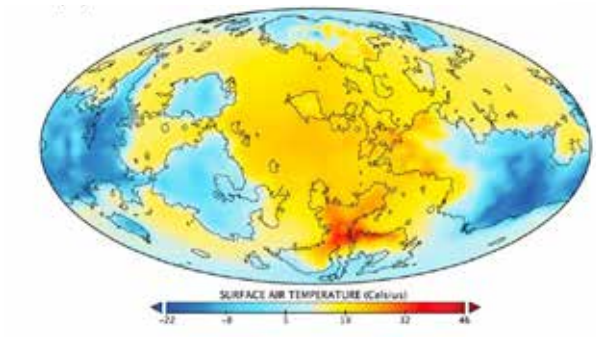

Cloudiness

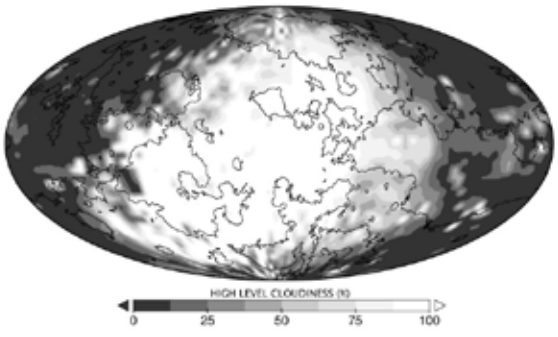

- Global mean surface air temperature of 11° C despite an incident solar flux at Venus's orbit ~46% higher than that received by modern Earth
- This is the result of this world's slow rotation which generates a strong circulation with rising motion and accompanying high thick clouds on the dayside that reflect a substantial fraction of the incident sunlight.

Surface level winds

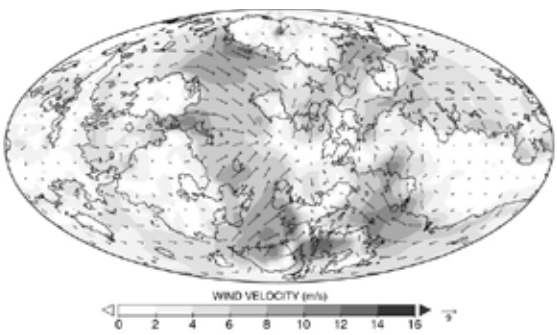

Rotation period >> Radiative time constant

(Earth : 100 Earth days)

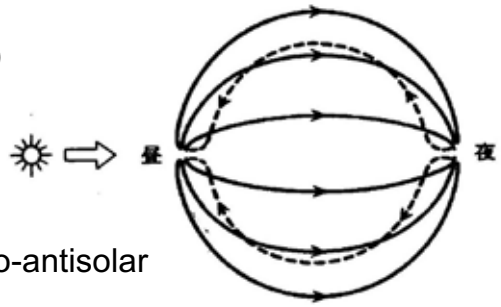

Subsolar-to-antisolar circulation

（松田 2000）

Rotation period << Radiative time constant

(Venus : 50 Earth years)

Axi-symmetric circulation

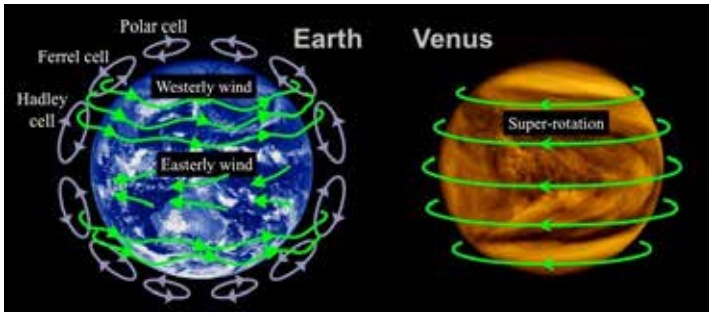

Ancient Martian climate: clue to the outer edge of the habitable zone

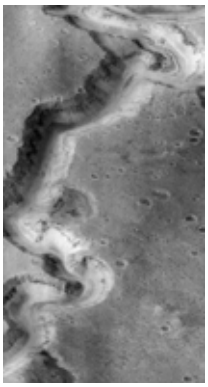

Valley network distribution (Ramirez & Craddock 2018)

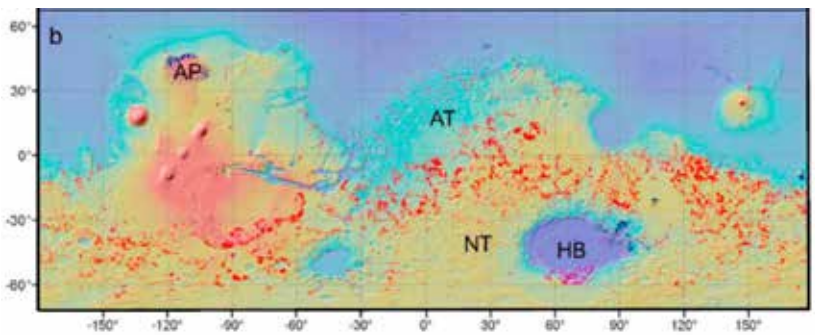

Can the ancient Mars be warm with CO_2 greenhouse effect ?

Kasting (1991)

- The ancient Sun was 25% dimmer than the present
- CO_2 greenhouse has been expected to warm the ancient Mars

- Warm lower atmosphere causes convection, which induces condensation of CO_2 in the upper atmosphere. The associated latent heating raises the temperature at upper levels, and at the same time cools the lower atmosphere so that the net energy balance is maintained.

Effect of CO_2 condensation

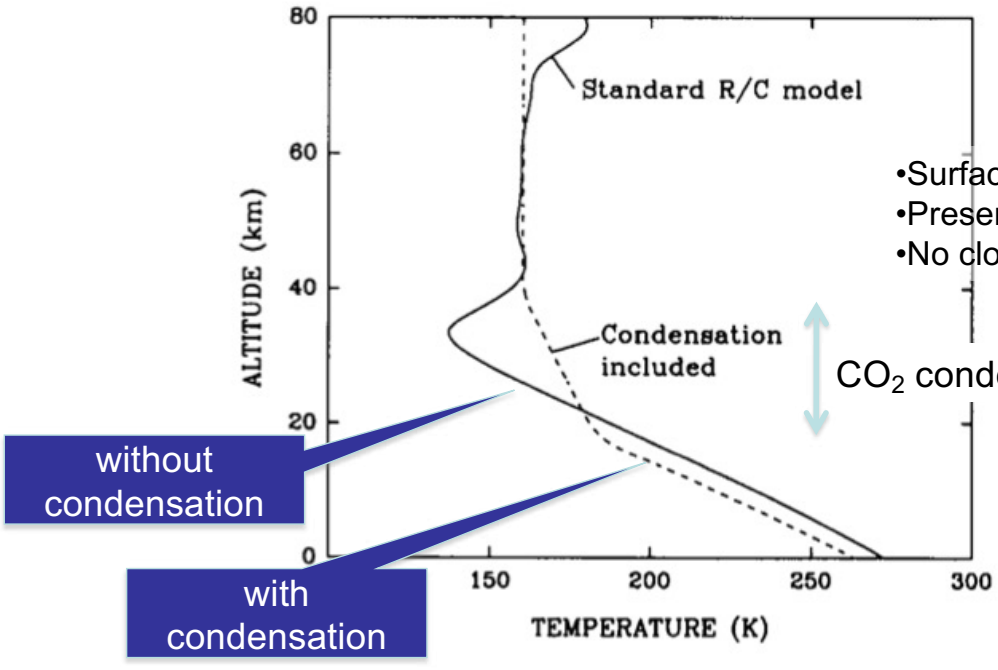

•Surface pressure of 2 bar
•Present solar constant
•No cloud albedo

CO_2 condensation

without condensation

with condensation

→When the solar constant is less than 86% of the present value, the surface temperature cannot exceed 273 K.

Greenhouse effect due to CO_2 ice clouds

Forget & Pierrehumbert (1997)

- CO_2 ice clouds scatter infrared radiation emitted from the surface, thereby causing greenhouse effect.
- CO_2 ice clouds also have cooling effect via increase of the planetary albedo. However, thick CO_2 atmosphere itself has a high albedo even when no cloud exists, and thus the effect of cloud albedo is relatively minor.
  - For example, cloud-free 2-bar CO_2 atmosphere has an albedo of 0.38. Addition of CO_2 clouds increases the albedo to 0.65, thereby reducing the solar absorption by 40%. At the same time the clouds absorbs 60% of the infrared radiation emitted from the surface.

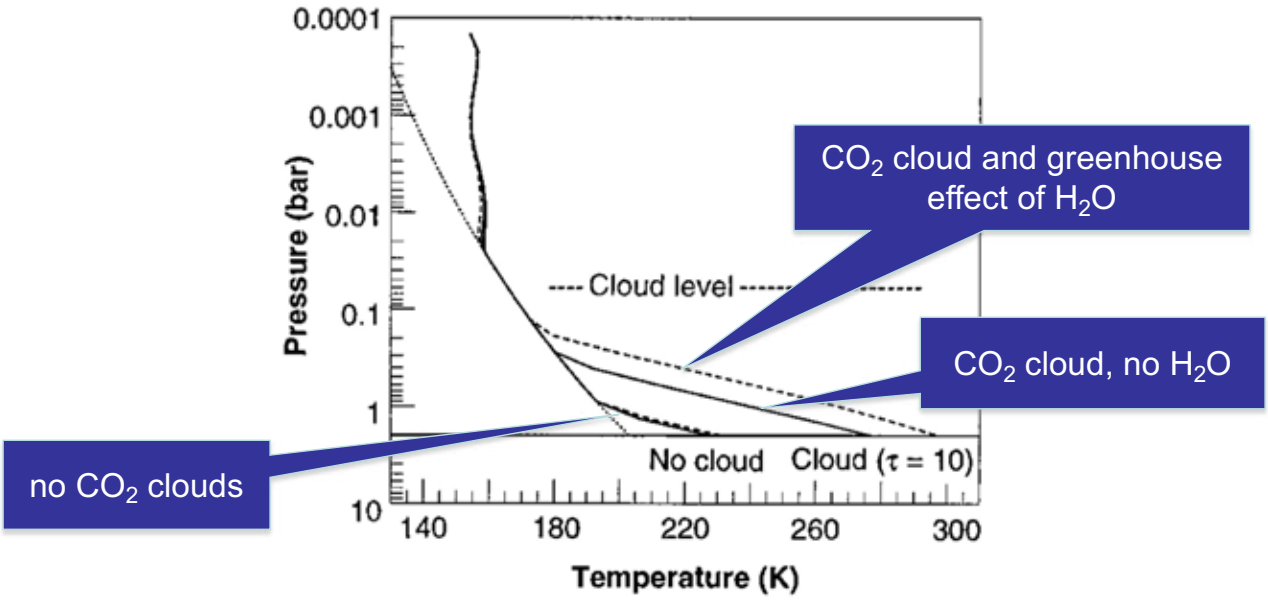

Fig. 2. Calculated mean temperature profiles for a 2-bar CO_2 atmosphere, assuming a 25% reduced solar luminosity corresponding to the early Mars conditions. The effect of the cloud from Fig. 1 (τ = 10, r = 10 μm) is shown in the cases of a wet (fully saturated troposphere; dashed curves) and a dry (solid curves) atmosphere. The dotted curve shows the CO_2 condensation temperature profile.

3D modelling of the early Martian climate under a denser CO_2 atmosphere: Temperatures and CO_2 ice clouds

(Forget et al. 2013)

- 3D global climate simulations of the early martian climate performed assuming a faint young Sun and a CO_2 atmosphere with surface pressure between 0.1 and 7 bars
- Previous studies had suggested that CO_2 ice clouds could have warmed the planet thanks to their scattering greenhouse effect. However, even assuming parameters that maximize this effect, it does not exceed +15 K. As a result, a CO_2 atmosphere could not have raised the annual mean temperature above 0° C anywhere on the planet.
- This is consistent with a cold early Mars scenario in which nonclimatic mechanisms must occur to explain the evidence for liquid water.

Mean surface temperature vs. Surface pressure (column CO_2 amount)

- Surface temperature increases up to 2 bar. Above 2–3 bar, Rayleigh scattering by CO_2 gas more than compensates for the increased thermal infrared opacity of the atmosphere. Increasing the atmospheric thickness does not result in an increase of the mean surface temperature.
- Taking into account the radiative effect of CO_2 ice clouds results in a global warming of the surface by more than 10 K resulting from the CO_2 ice cloud scattering greenhouse effect.
- The collapse of the atmosphere into permanent CO_2 ice caps is predicted for pressures higher than 3 bar.

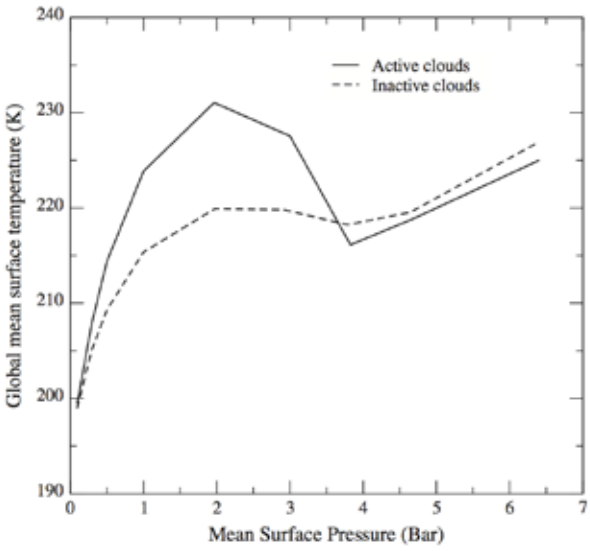

Fig. 1. Global mean annual mean surface temperature (K) as a function of surface pressure in our baseline simulations (obliquity = 25°, [CCN] = 10^5 kg^{-1}, circular orbit) with and without radiatively active CO_2 ice clouds.

An example of the instantaneous CO_2 ice clouds coverage for a mean surface pressure 2 bar

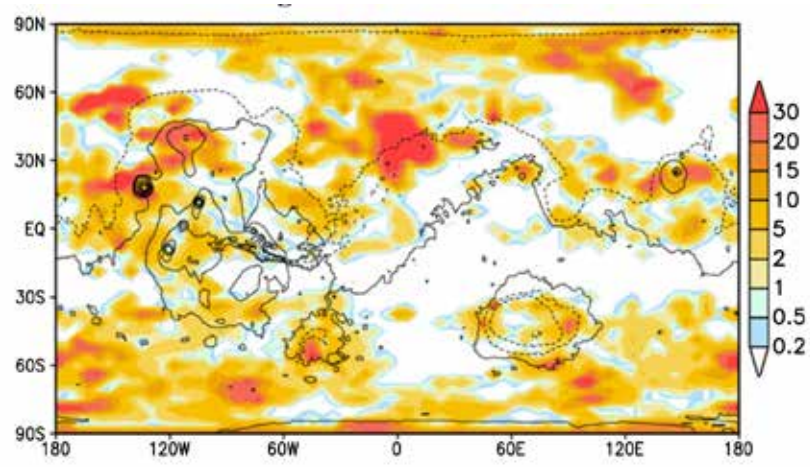

- CO_2 ice clouds cover a major part of the planet but not all. Their behavior is controlled by a combination of large scale ascents and descents of air, stationary and travelling waves, and resolved gravity waves related to the topography.
- The mean cloud warming remains lower than 15 K because of the partial cloud coverage and the limited cloud optical depth.

H_2–CO_2 greenhouse ? (Ramirez et al. 2014)

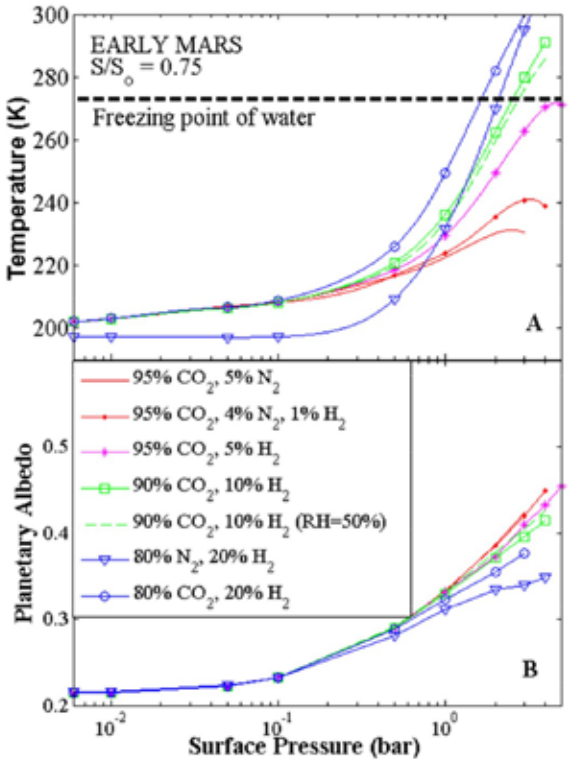

Collision-induced absorption (CIA) band of H_2 caused by the foreign-broadening by the background CO_2 atmosphere

Reduced mantle conditions could have favored enhanced outgassing of H_2 over long timescales. Hydrogen is continuously replenished by volcanism that offsets losses to space.

An atmosphere containing -4 bar of CO_2 and 5% H_2 would have brought Mars' average surface temperature up to the freezing point of water.

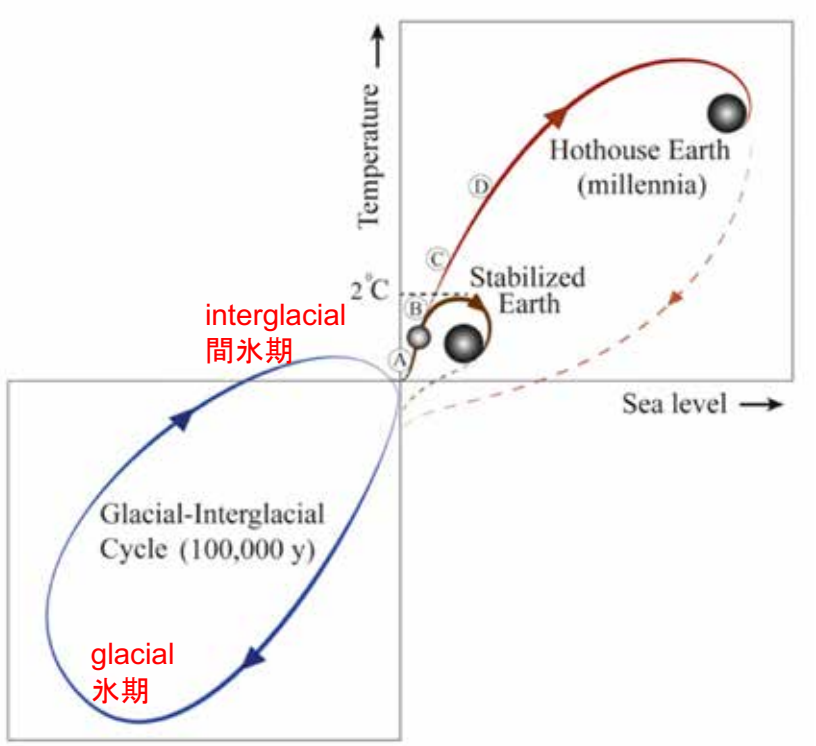

Steffen et al. (PNAS, 2018)

Milankovitch cycle

from Wikipedia

low summer insolation in the northern high latitude → growth of ice sheets → glacial inception (ice age)

Precession 歳差

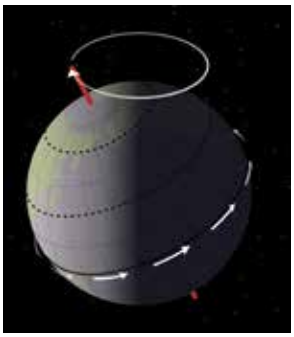

Obliquity 自転軸傾斜角

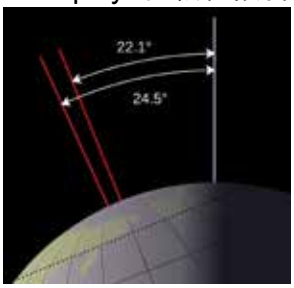

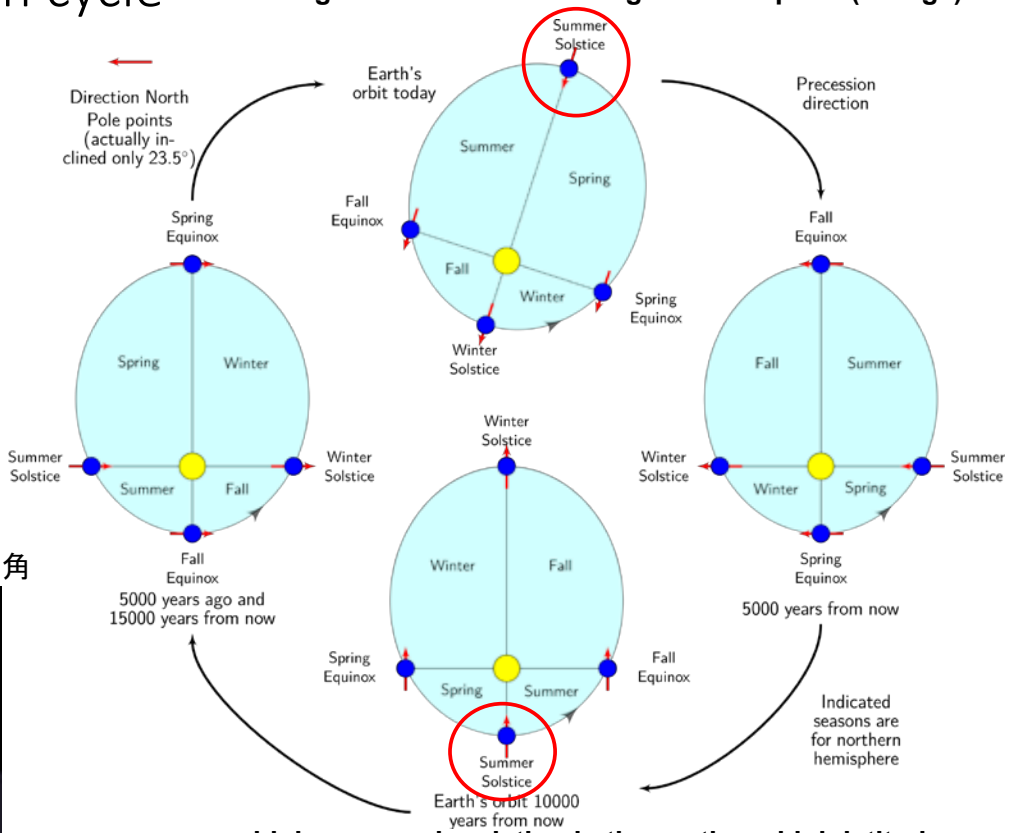

high summer insolation in the northern high latitude → decay of ice sheets → Interglacial (warm interval)

Milankovitch cycles on Mars and Earth

Table 12.10 The orbital elements of Mars and the Earth and their variability.

		Martian variability			Terrestrial variability	
Parameter	Present Mars	Range	Cycle (years)	Present Earth	Range	Cycle (years)
Obliquity (°)	25.19	0–85*	120 000**	23.45	22–24	41 000
Eccentricity	0.093	0–0.12	120 000***	0.017	0.01–0.04	100 000
Longitude of perihelion (°)	250	0–360	51 000	285	0–360	21 000

* Before ~10 Ma, obliquity variations are chaotic. While unpredictable at an exact time, statistically they would have varied between 0 and 85° (Laskar *et al.*, 2004; Touma and Wisdom, 1993).
** The amplitude of obliquity oscillation is modulated with a ~1.2 Myr period envelope.
*** The amplitude of eccentricity oscillation is modulated with a ~2.4 Myr period envelope.

Catling & Kasting 2017

Milankovitch cycles on Mars

自転軸傾斜角

軌道離心率

北極域の夏至の日射

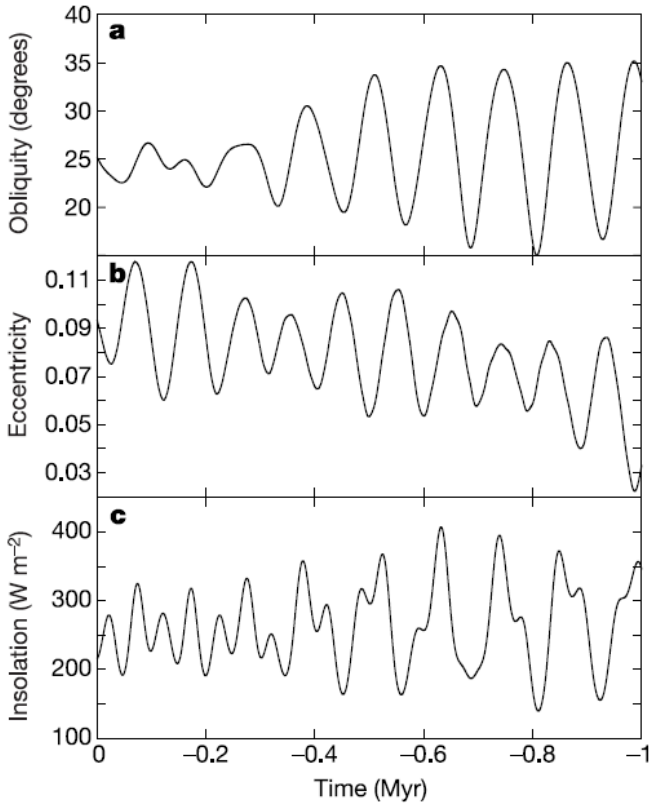

Laskar et al. (2002)

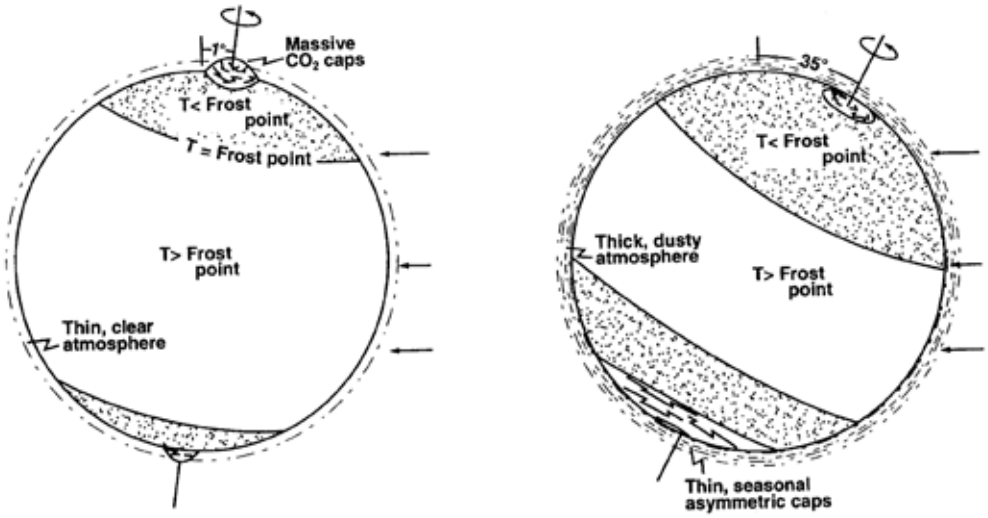

- low obliquity → cold pole → massive polar cap → dry atmosphere → retreat of ice sheet

- high obliquity → warm pole → thin polar cap → moist atmosphere → growth of ice sheet, ice accumulation in the tropics

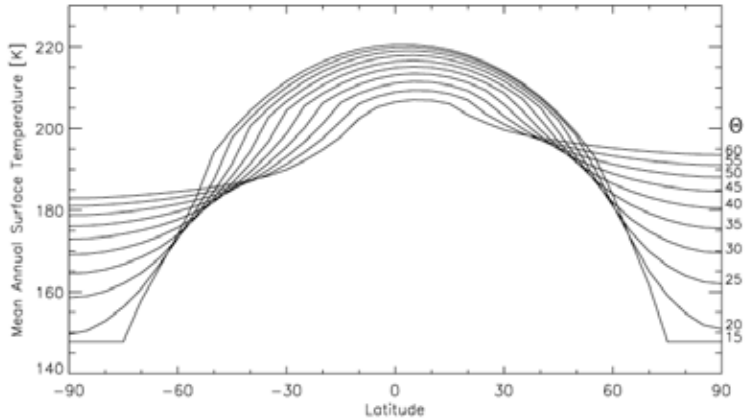

Figure 3. Mean annual surface temperature for a range of obliquities. The eccentricity is 0.12, and the L_S at which perihelion occurs is 270, corresponding to southern summer. A thermal inertia of 250 J m^{-2} s$^{-1/2}$ K^{-1}, an albedo of 0.25, a surface pressure of 600 Pa, and an infrared dust opacity of 0.1 are assumed. Discontinuities in the slope of each curve are due to the effects of seasonal CO_2 frost.

Mellon & Phillips (2001)

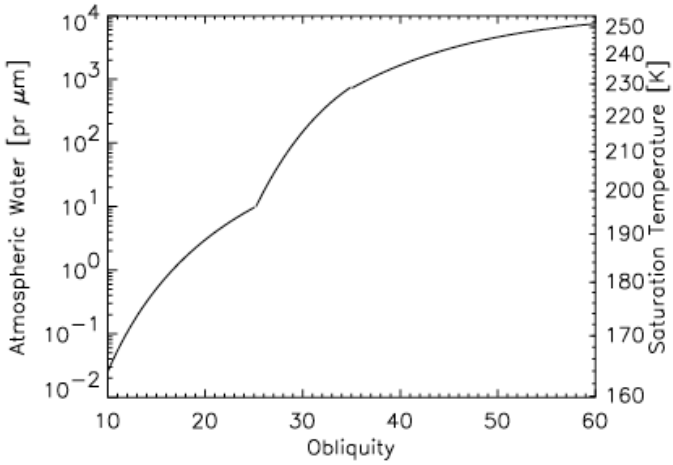

recurrent slope lineae

- transition between different climate regimes ?

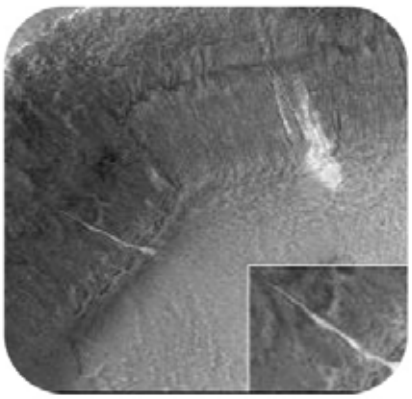

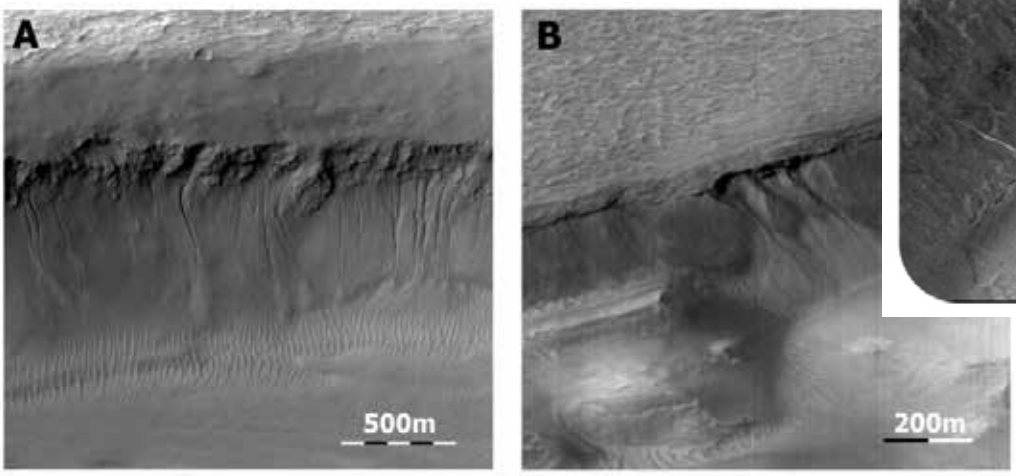

Buried glaciers

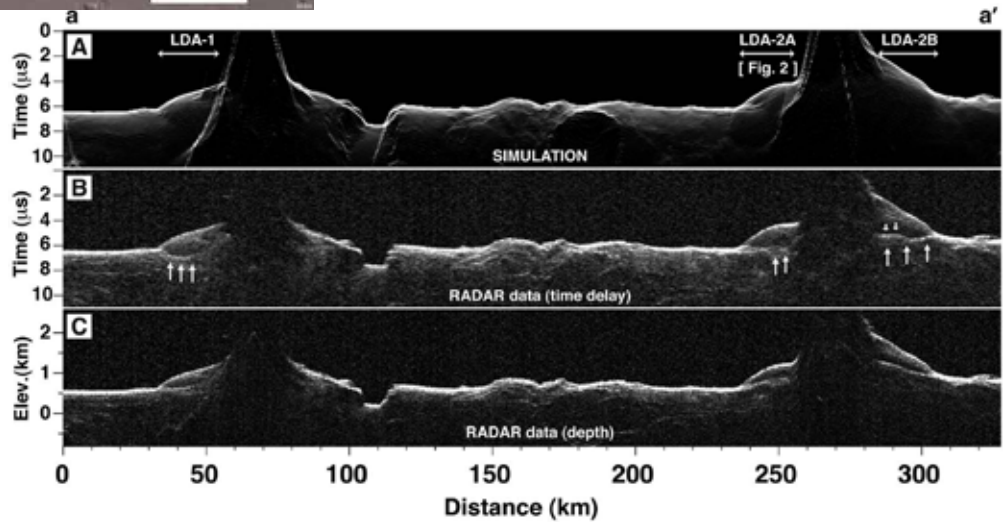

Formation of glaciers on Mars by atmospheric precipitation at high obliquity Forget et al. (2006)

- The model predicts ice accumulation in regions where glacier landforms are observed, on the western flanks of the great volcanoes and in the eastern Hellas region

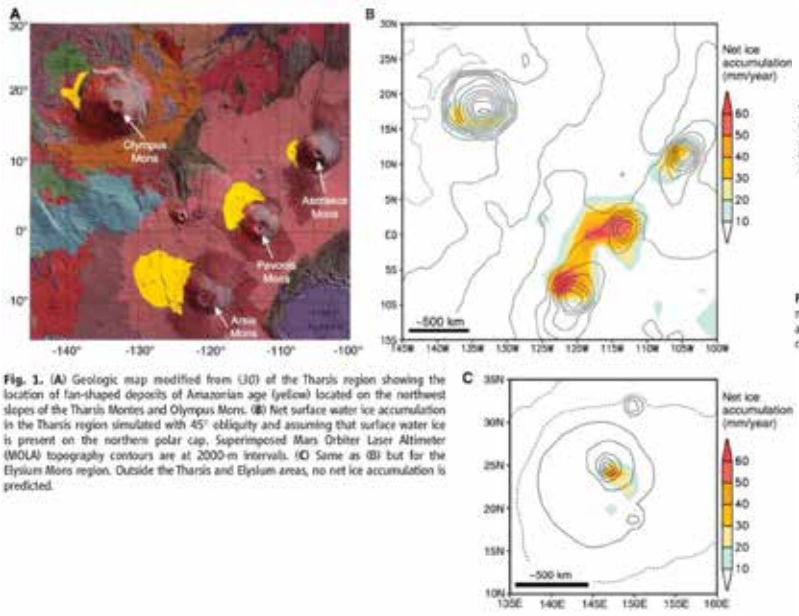

Fig. 1. (A) Geologic map modified from (30) of the Tharsis region showing the location of fan-shaped deposits of Amazonian age (yellow) located on the northwest slopes of the Tharsis Montes and Olympus Mons. (B) Net surface water ice accumulation in the Tharsis region simulated with 45° obliquity and assuming that surface water ice is present on the northern polar cap. Superimposed Mars Orbiter Laser Altimeter (MOLA) topography contours are at 2000-m intervals. (C) Same as (B) but for the Elysium Mons region. Outside the Tharsis and Elysium areas, no net ice accumulation is predicted.

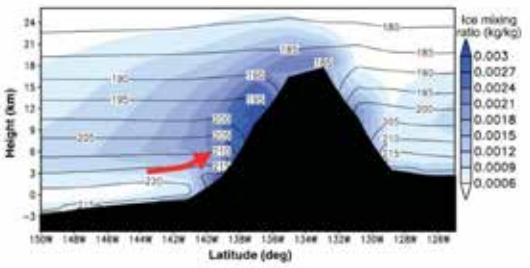

Fig. 3. Cross section of Olympus Mons along the 16°N latitude showing the mean atmospheric ice mass mixing ratio (shaded blue) and the atmospheric temperature (contour, K) averaged over the period of ice accumulation Ls = 125° to 155° (northern summer). The strong northwesterly winds induce adiabatic cooling on the flank of the volcanoes and atmospheric condensation and precipitation.

Venus:

Massive eruptions several hundred million years ago ?

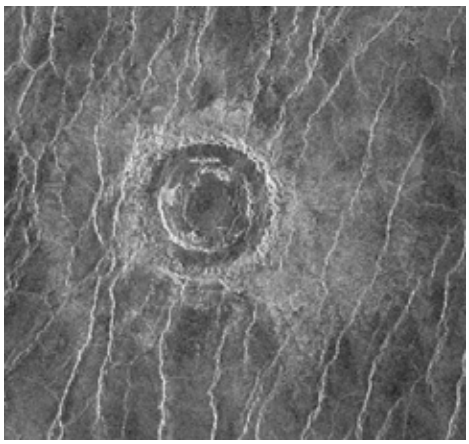

Radar image of Venus surface by NASA's Magellan spacecraft

Wrinkle ridges may have been formed by thermal stress caused by a sporadic enhancement of greenhouse effect (H_2O) in the past. (Bullock and Grinspoon, 2001)

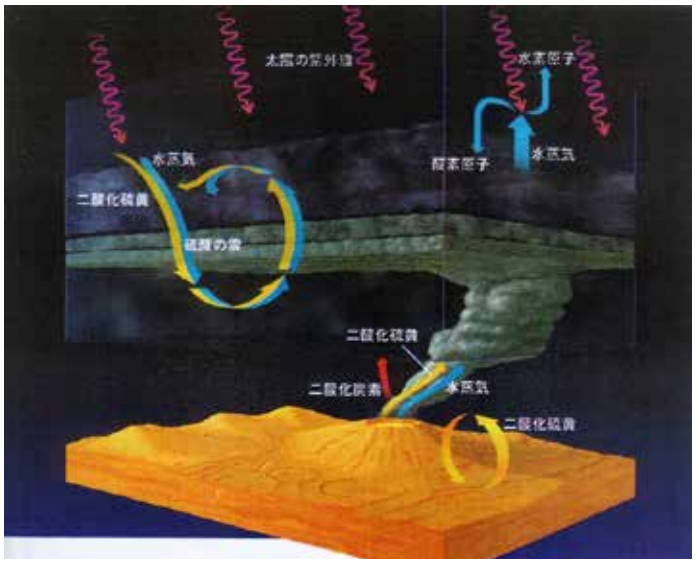

Decadal variation of Venusian atmosphere

SO_2 above Venusian clouds (Marcq et al. 2013)

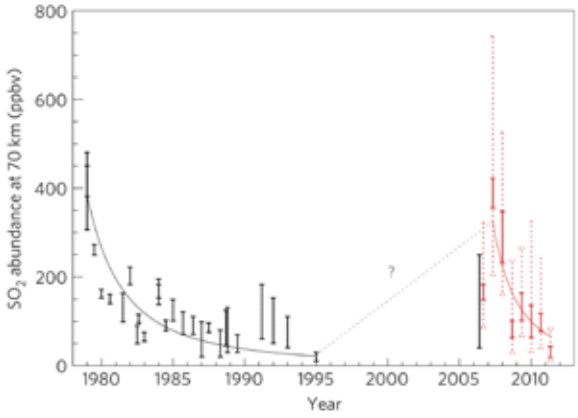

Figure 3 | More than thirty years of SO_2 measurements at Venus's cloud top. Black stands for previously published measurements[26]. Red stands for the 8-month moving average of the retrievals also shown in Fig. 1. Solid red error bars represent 1σ random uncertainty, and dotted red error bars represent measurement dispersion in each temporal bin.

UV albedo (Lee et al. 2019)

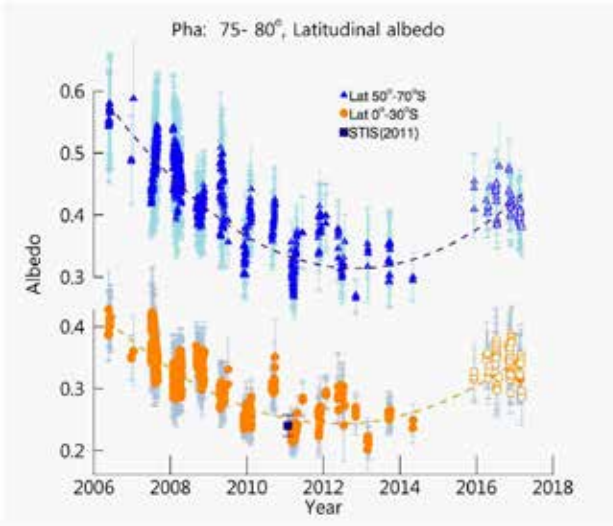

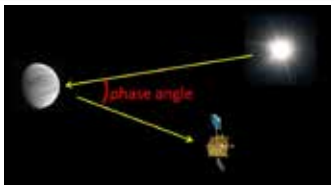

Correlation between UV contrast and SO_2 density (Lee et al. 2015)

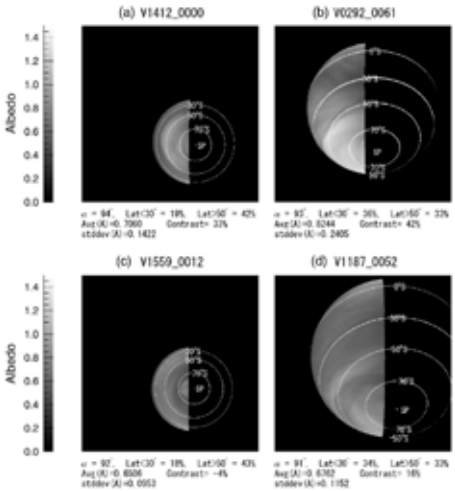

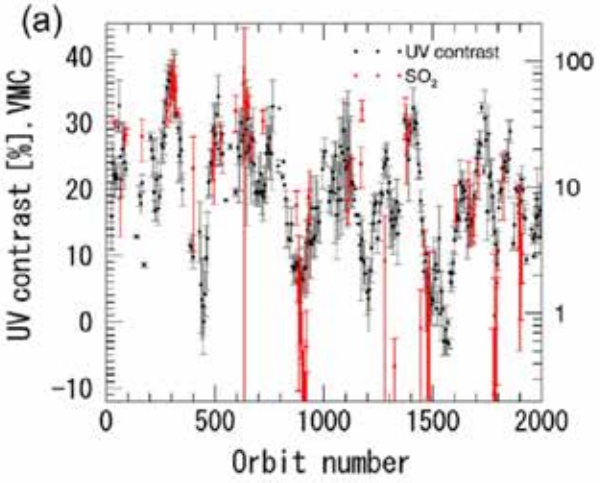

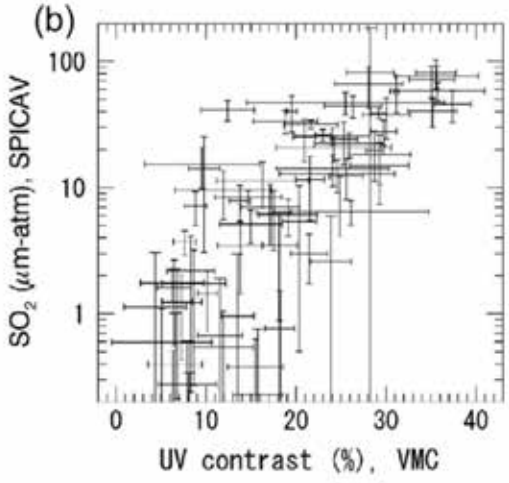

long-term variation of zonal wind (Khatuntsev et al. 2022)

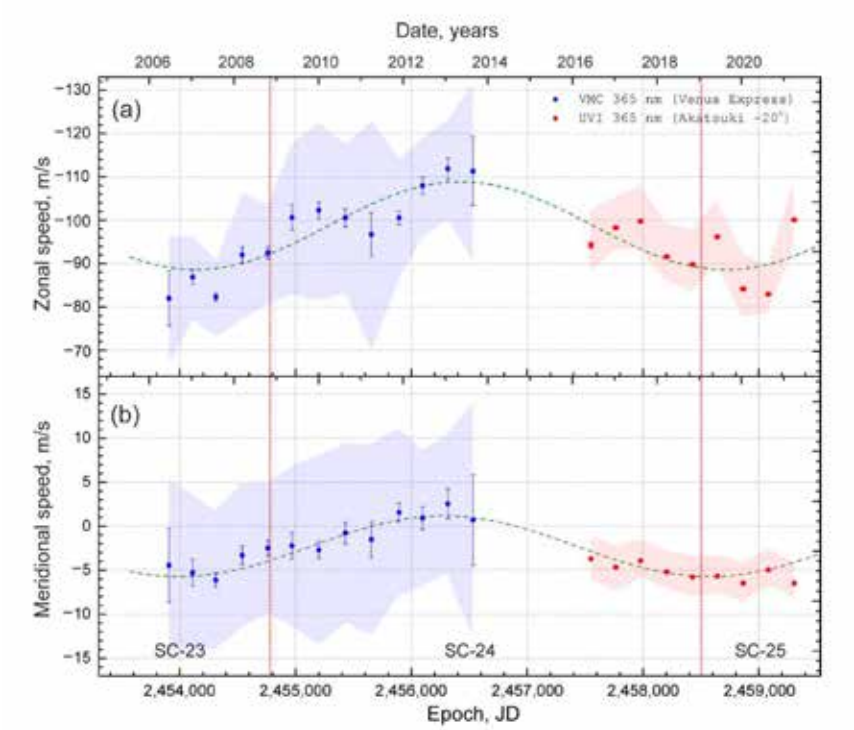

Long-term variation of the Venus atmosphere revealed by Akatsuki cameras

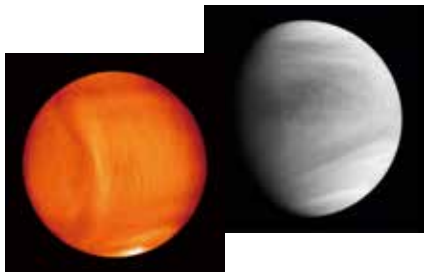

Watanabe (2023, master's thesis)

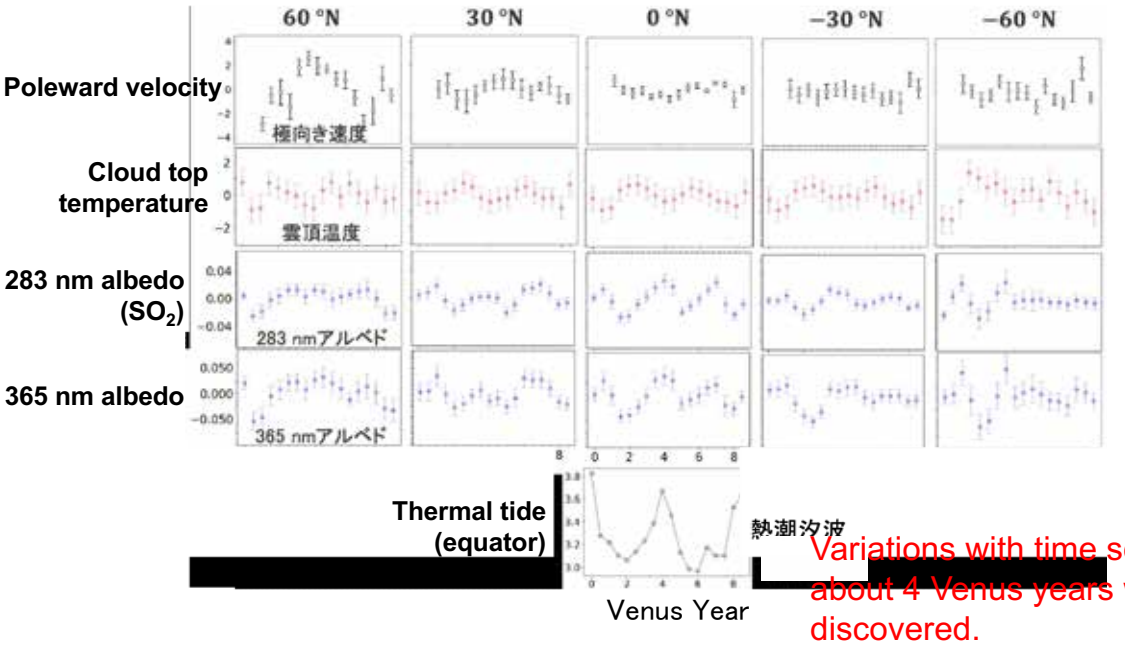

Variations with time scales of about 4 Venus years were discovered.

Understanding the diversity in a multi-dimensional parameter space

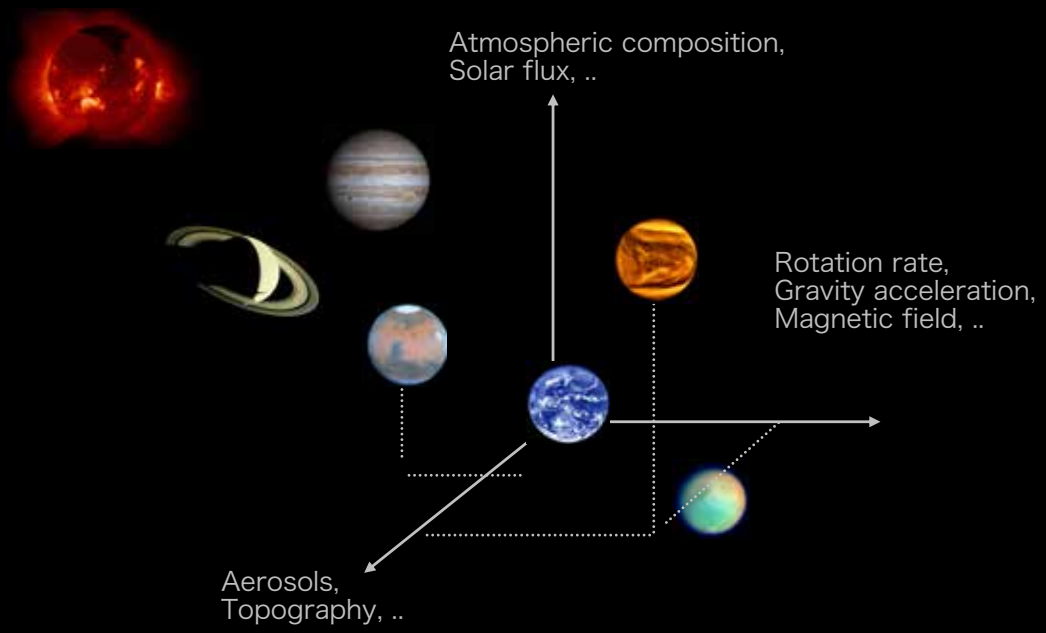

Giant exoplanet with a hot upper atmosphere (Evans et al. 2017)

- Secondary eclipse of WASP-121b using the HST Wide Field Camera 3 (WFC3)
- If upper layers are cooler than lower layers, molecular gases will produce absorption features in the planetary thermal spectrum. Conversely, if there is a stratosphere—where temperature increases with altitude—these molecular features will be observed in emission.

Lammer et al. (2013)

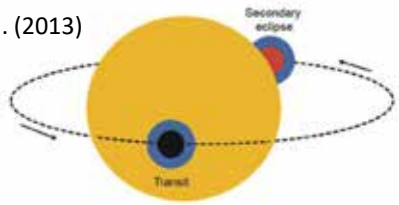

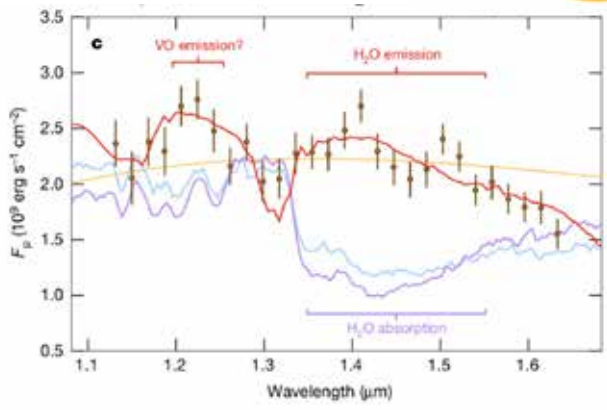

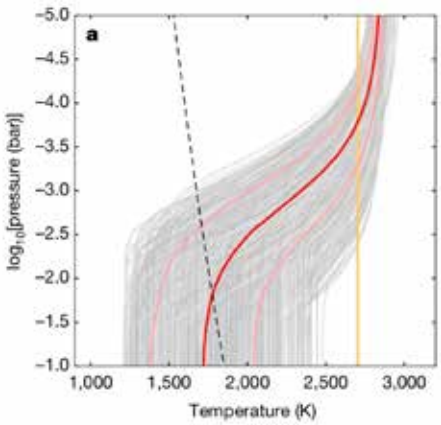

Figure 3 | Temperature–pressure profiles for WASP-121b. a, Grey lines show a random subset of T–P profiles sampled by the MCMC retrieval analysis. Red line shows the median temperature at each pressure level, and pink lines show ranges either side encompassing ±34% of the sampled profiles. Yellow line indicates the best-fit isothermal temperature of

Meadows et al. (2018)
ASTROBIOLOGY, Vol 18

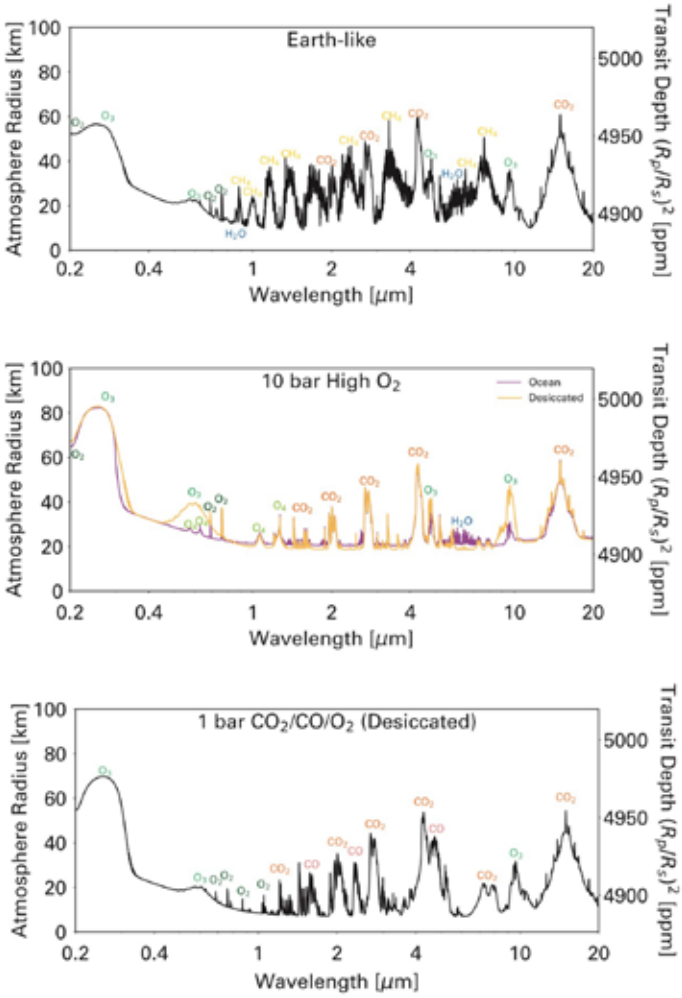

FIG. 6. Transit transmission spectra of potential planetary environments with different O_2 abundances for planet orbiting the M5.5V star Proxima Centauri (Meadows *et al.*, 2018). Illustrating spectral features that can help distinguish photosynthetic from abiotically generated O_2 in a planetary atmosphere. From top to bottom: self-consistent Earth-like atmosphere with 50% cloud cover (21% O_2); 10 bar abiotic O_2 (95% O_2) atmosphere produced by early ocean loss with ocean remaining (purple) and desiccated (orange); 1 bar desiccated CO_2/CO/O_2 atmosphere that has reached a kinetic–photochemical equilibrium between the photolysis rate of CO_2 and kinetics-limited recombination (15% O_2). Effective atmospheric radius in kilometers is on the left *y* axes and transit depth is shown on the right *y* axes. The photosynthetic source for O_2 in the Earth-like case is made more likely by the presence of O_2/O_3, water, and methane. High O_2 cases with and without water are distinguished by the presence of O_4, and the behavior of the 0.5–0.7 μm Chappuis band that is sensitive to tropospheric O_3, which is more abundant in the desiccated case. The desiccated chemical equilibrium atmosphere is easily distinguished by its high levels of CO.